Hall anomaly of diffusive magnetic waveguides

A. Nogaret,[1,*] D. N. Lawton,[1] D. K. Maude,[2] J. C. Portal,[2] and M. Henini[3]
[1]*Department of Physics, University of Bath, Claverton Down, Bath, BA2 7AY, United Kingdom*
[2]*High Magnetic Field Laboratory CNRS–MPI, 25 Avenue des Martyrs, 38042 Grenoble CEDEX 9, France*
[3]*School of Physics and Astronomy, University of Nottingham, Nottingham NG7 2RD, United Kingdom*
(Received 12 September 2002; revised 21 January 2003; published 24 April 2003)

We report on the Hall resistance in a diffusive two-dimensional (2D) electron channel incorporating a strong magnetic barrier at its center. An external magnetic field was tilted in the plane perpendicular to the barrier to separate magnetization effects due to ferromagnetic elements from effects of magnetic channeling in the 2D electron gas. In the presence of an inhomogeneous current distribution, the Hall resistance is found to measure the trapping of electrons in or out of magnetic edge states rather than the magnetization average over the Hall cross. A simple formula for the Hall resistance in this regime is proposed.

DOI: 10.1103/PhysRevB.67.165317 PACS number(s): 73.23.−b, 85.75.Nn, 75.75.+a

Hall probes are increasingly being used to investigate mesoscopic magnetism[1] and superconductivity[2] and in the design of novel magnetoelectronic devices.[3] A small ferromagnetic or superconducting element fabricated at the surface of a Hall cross—usually containing a two-dimensional electron gas (2DEG)—generates an inhomogeneous magnetic field that locally deflects electron trajectories and somehow modifies the Hall voltage across the whole channel. The magnetization of Ni and Al dots[1] was measured under the assumption that the Hall resistance is proportional to the magnetization averaged over the Hall cross. This intuitive formula was later justified theoretically for diffusive[4] and weakly modulated ballistic devices.[5] In contrast, strongly modulated systems where the cyclotron radius is smaller than the width of the magnetic barrier[5] or the magnetic correlation length[6] are dominated by edge-state transport. A transition from sheet to edge transport was demonstrated through the saturation of the Hall resistance across tunable spots of magnetic field.[7] This Hall anomaly is a ballistic geometrical resonance comparable to the last Hall plateau observed in earlier electron billiards.[8,9]

In this paper, we investigate a magnetic waveguide consisting of a dysprosium stripe that produces a strong magnetic barrier at the center of a 2DEG. One obvious advantage of single stripes over lateral superlattices[10] is that the modulation potential affects the Hall resistance. A Hall anomaly is reported that is enhanced in dirty 2DEG's. To distinguish between effects due to the stripe magnetization curve (dependent on the total applied magnetic field B) and magnetic channeling at the edges of the magnetic barrier (dependent on the normal vector component of the applied field B_z), we tilted the external magnetic field normal to the stripe. The Hall anomaly was found to scale remarkably well with B_z while shifting over two orders of magnitude in B, thus demonstrating its channeling origin. The resistivity tensor was calculated across realistic magnetic barrier profiles to evaluate the effect of the reduction in the mean free path. We found that magnetic edge states become increasingly localized in regions of high magnetic gradient, which, in our sample geometry, are disconnected from the Hall probes. The Hall anomaly thus measures the trapping and untrapping of electrons out of magnetic edge states. A simple formula for the Hall resistance is derived that is in good agreement with experimental data.

The devices studied here are narrow $Al_{0.3}GaAs/GaAs$ channels with a dysprosium stripe fabricated at their center whose length can be considered as infinite for most practical purposes. The cross section and dimensions are shown in Figs. 1(a) and 1(b). The magnetic waveguide was completed by fabricating a top metal gate covering the active channel area including the stripe.[11] Our shallow 2DEG was formed by δ doping the center of a quantum well lying 24 nm below the surface. Such a short distance between the stripe and the 2DEG minimized the decay of the stray magnetic fields at the site of the 2DEG. In return, the 2DEG mobility was rather modest with $\mu = 3.6\times10^5$ cm^2 V^{-1} s^{-1} for an electron density $n_s = 3.4\times10^{11}$ cm^{-2}. Biasing the gate in the ±0.2 V range changed the mobility over an order of magnitude while tuning the electron concentration by 10%. The resistance effects reported below were enhanced at low mobilities; therefore, all measurements were taken at a negative gate bias of -0.2 V. Transport is thus diffusive with a mean free path of $l = 1.1$ μm smaller than both the 2 μm channel width and the voltage probe separation of 8 μm.

The device was cooled down to 1.3 K in the variable-temperature insert of a superconducting magnet and rotated *in situ* about the axis of the stripe. The accuracy of the tilt angle was $\pm0.8°$, representing the maximum discrepancy between direct readings on the rotation probe caliper, the $\cos\theta$ dependence of the Hall resistance, and the Shubnikov—de Haas peaks at high magnetic field. Figures 1(a) and 1(b) show the stray fields threading the stripe when it is magnetized normal, $\theta=0°$, and in the plane of the 2DEG, $\theta=90°$. Electrons in the 2DEG only sense to the normal component of the stray fields that form a rectangular barrier at $\theta=0°$ evolving towards a triangular barrier at $\theta=90°$. Since the magnetization depends on the total magnetic field, the dependence of the Hall resistance on θ determines whether the Hall resistance measures the average magnetization or the channeling by microscopic magnetic gradients.

The raw Hall curves show a departure from the usual linear trend which is indicated by the grayed area in the inset

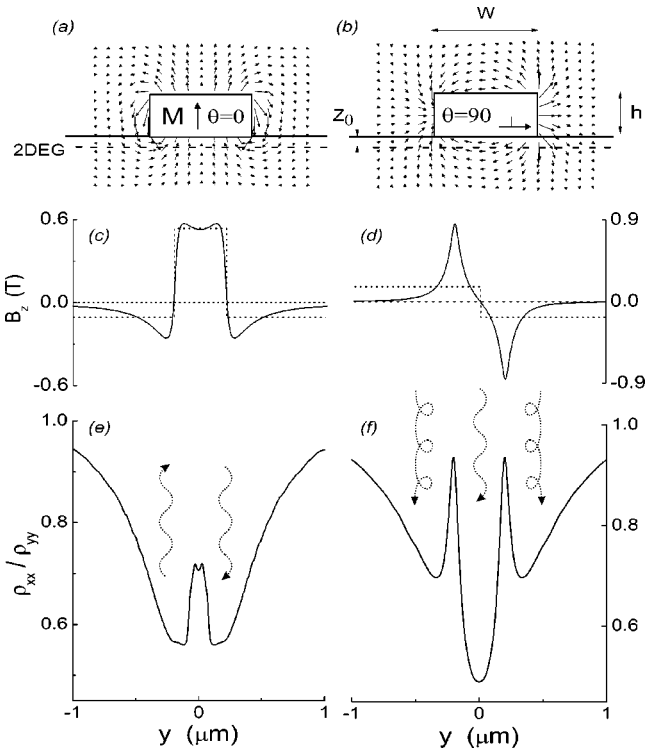

FIG. 1. Cross section of the electron channel showing the stray magnetic fields emanating from the Dy stripe when its magnetization is (a) normal and (b) in the plane. The current is applied parallel to the stripe. (c), (d) The magnetic barriers at the site of the 2DEG (solid lines) and their rectangular approximation (dotted lines). (e), (f) The resistivity tensor anisotropy calculated using the velocity-velocity correlation function in the exact barrier profiles shown above. Dips in ρ_{xx}/ρ_{yy} indicate channeling by snake and cycloid orbits in the regions of high magnetic gradient. Plots (c), (d), (e), (f) show the full channel width of 2 μm whereas plots (a), (b) only extend ± 0.5 μm away from the center. $w=400$ nm, $h=140$ nm, $z_0=24$ nm, and $\tau=2$ ps.

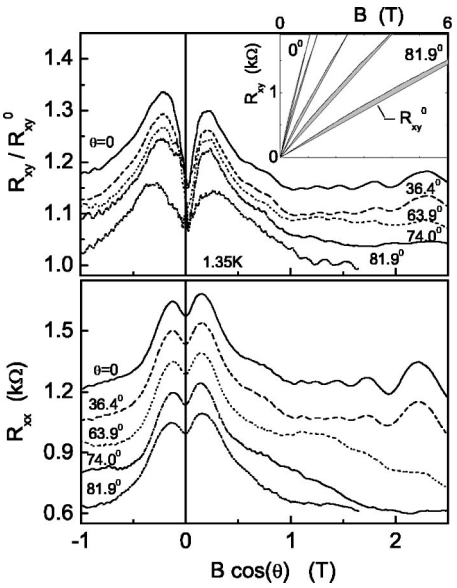

FIG. 2. Top panel: the Hall resistance upon the extrapolated Hall resistance plotted against the normal component of the applied magnetic field for several values of the tilt angle. For clarity, curves were vertically offset by 0.02. Deviations from the linear Hall behavior are shown by the grayed areas in the inset. Lower panel: the longitudinal resistance also plotted against $B_z=B\cos\theta$ (curves vertically offset by 150 Ω).

to Fig. 2. Note that this superlinear behavior shifts to higher *total* magnetic fields as the tilt angle increases. The Hall resistance returns to its usual linear trend at $B_z>1$. This trend extrapolated to the origin was used to define the Hall resistance of the unmodulated device, R_{xy}^0. The ratio R_{xy}/R_{xy}^0 exhibits a peak that increases from $B=210$ mT at $\theta=0°$ up to $B=8.35$ T at $\theta=89°$ (not shown). Replotting these curves as a function of $B_z=B\cos\theta$ instead of B, as done in the top panel of Fig. 2, reveals that the peak position at $B_z\approx 0.210$ T remains broadly independent of the tilt angle. More generally, the resistance structure at $B_z<1$ T is independent of θ while, at $B_z>1$ T, $R_{xy}/R_{xy}^0\approx 1$. This invariance might suggest that the shape of the magnetic barrier is constant. This idea can be dismissed by examining the R_{xy}/R_{xy}^0 curves at $B_z>1$ T. The Hall plateaus in the $\theta=0°$,36.4° curves are dampened at $\theta=63.9°$ and become completely suppressed at higher tilt angles. This is because degenerate Landau levels will form in the flat regions of the square magnetic barrier [see Fig. 1(c)], since the magnetic length $\sqrt{\hbar/eB_z}\approx 35$ nm is much less than the barrier width. In contrast, the triangular magnetic barrier of Fig. 1(d) lifts the Landau degeneracy. This leads to the formation of current carrying states following the lines of constant magnetic field. In this respect, it is interesting to note that the quenching of the Shubnikov–de Haas oscillations in the $\theta=63.9°$ and 74.0° curves of the lower panel is accompanied by a drop in R_{xx}. Overall, R_{xx} and R_{xy}/R_{xy}^0 present the same structure that scales with B_z.

The peak has two possible origins described in Fig. 3. Case I assumes that the Hall resistance measures the magnetization average. Any nonlinearity in R_{xy} must therefore occur at a fixed value of B because spins align with the total applied magnetic field. For example the magnetization saturates at a value of $B=B_s$ which is independent of the direction in which B is applied.[12] The induced structure at $B=B_s$ in R_{xy} is therefore independent of θ.[13] In case II, we consider the effect of electrons channeled at the edge of the magnetic barrier. At $B_z<B_m$ and $B_z>B_m$, the Hall resistance is reduced due to the trapping of a fraction of electrons into snake states (1) and cycloid states (3) that do not reach the Hall probes. The Lorentz force does not deflect these electrons; hence, they are not accounted for in the Hall voltage. Instead they are released by increasing B_z. We have numerically integrated Newton's equation of motion for an electron departing at an angle φ from the line of zero magnetic field in the triangular barrier of Fig. 1(d). We found that snake trajectories correspond to $\varphi<+61°$ which represents one-third (61°/180°) of the Fermi surface.[14,15] Figure 3 shows that a Hall resistance peak is expected at a constant value of $B_z=B\cos(\theta)=B_m$. Following previous theoretical works,[16,17] we calculate the amplitude of the negative modulation, B_m, by averaging the negative modulation field of the

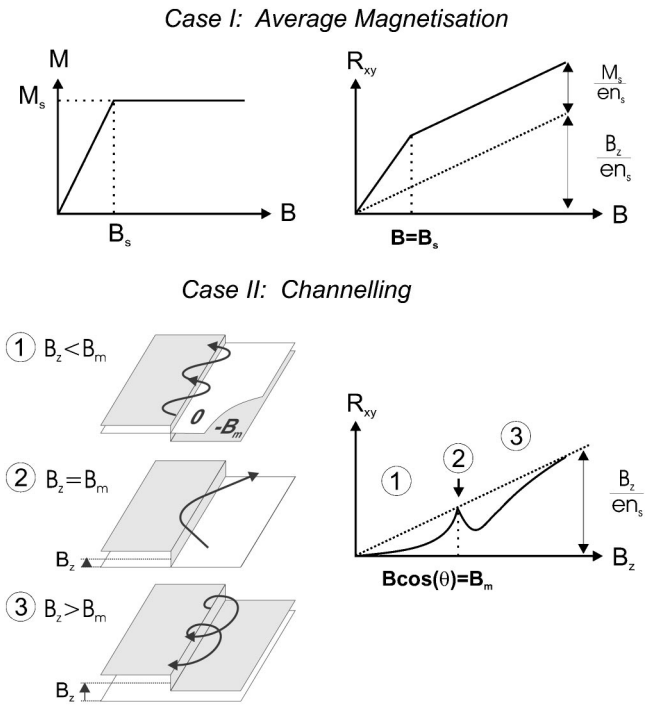

FIG. 3. The Hall resistance under the assumption that it measures the average magnetization $M(B)$ (case I) and under the assumption that it measures channeling by magnetic edge states (case II). The edge of the magnetic barrier (gray surface) and electron trajectories are shown at three values of B_z. Here B_m is the amplitude of the negative modulation.

barriers in Figs. 1(c) and 1(d) (dotted curves). We find $B_m = 0.173$ T at $\theta = 0°$ and $B_m = 0.148$ T at $\theta = 90°$. These values are in reasonable agreement with the R_{xy}/R_{xy}^0 peak position at 0.210 T. The small angular dependence of B_m also explains the peaks scaling with $B\cos(\theta)$. By contrast, if case I was true, the peak would occur at a constant value of B instead of shifting nearly two orders of magnitude. One therefore concludes that the Hall resistance measures channeling by magnetic edge states (case II) and not the average magnetization (case I).

One particular concern with this picture is the actual degree of inhomogeneity in the current distribution and why it should be enhanced in the diffusive regime. To answer this, we have calculated the local diffusion tensor as a function of the distance, y, from the center of the waveguide using the velocity-velocity correlation function.[18] Because snake electrons have a velocity periodic as a function of time,[19] we find more convenient to use the following expression for the diffusion tensor[20]:

$$D_{\mu,\nu} = \left\langle \frac{\int_0^T dt v_\mu(t) v_\nu(0) e^{-t/\tau}}{1 - e^{-T/\tau}} \right\rangle, \quad \mu,\nu \equiv x,y, \qquad (1)$$

where T is the period of the trajectory defined by the electron initial position and initial velocity angle at $t = 0$. All trajectories were calculated by integrating Newton's equation of motion in the exact barrier profiles of Figs. 1(c) and 1(d).

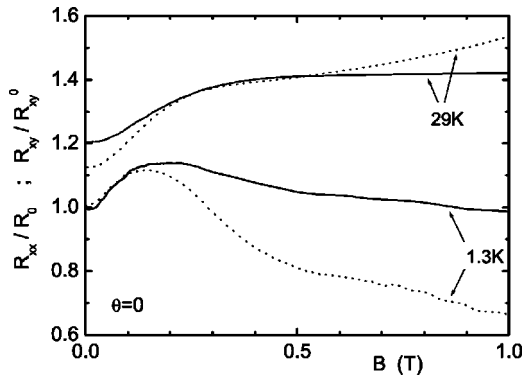

FIG. 4. R_{xy}/R_{xy}^0 (solid line) and R_{xx}/R_0 (dotted line) at 1.3 and 29 K (vertically shifted by $+0.4$).

The time integration and isotropic averaging over the Fermi surface was then computed numerically. The elastic scattering time $\tau = 2$ ps and the electron density were set as in the experiment. The tensor anisotropy $D_{yy}/D_{xx} \equiv \rho_{xx}/\rho_{yy}$ is plotted in Figs. 1(e) and 1(f) as a function of the position in the channel, y.

The results show dips in regions where the magnetic field gradient is the steepest. These correspond to the drift path of snake and cycloid orbits and appear more pronounced in the former because snake orbits carry a larger drift velocity. At $\tau = 2$ ps the drift paths are very neatly localized to small bands of the 2DEG running parallel to the magnetic barrier. Electrons trapped in these bands will be less likely to reach the Hall probes. When increasing the value of τ in our model we find that the drift paths become broader and overlap at about 8 ps. This is because electrons can travel larger distances before being scattered. The localization of drift paths thus explains the enhancement of the Hall anomaly in the diffusive regime.

We can now recall a simple general formula for the Hall resistance in the regime of strongly modulated magnetic fields.[21] Orbits that acquire a finite guiding center drift velocity v_d in a magnetic gradient add a diffusion term $\delta D_{xx} = \langle v_d^2 \rangle \tau$ to the Drude tensor. Einstein's equation then gives for the resistivity

$$\frac{R_{xy}}{R_{xy}^0} = \frac{R_{xx}}{R_0}, \qquad (2)$$

where R_0 is the Drude resistance. Figure 4 plots together the left and right terms of Eq. (2). At 1.3 K, these contain qualitatively the same structure. However, a vertical offset is also present that is mainly due to scattering by the diffuse sidewalls.[22] This parasitic resistivity component is suppressed by raising the temperature above 20 K. At 29 K, Eq. (2) is seen to be in excellent agreement with the data.

A last point to clarify is why snake states should exist at all in the first place. Dysprosium must have a sufficiently steep magnetization curve if the induced modulation profile is to change sign at $B_z \approx 0$. A soft ferromagnet would instead lead to a very different type of magnetoresistance saturation that was calculated by Reijniers and Peeters.[13] We now argue that the steep magnetization of dysprosium is because its

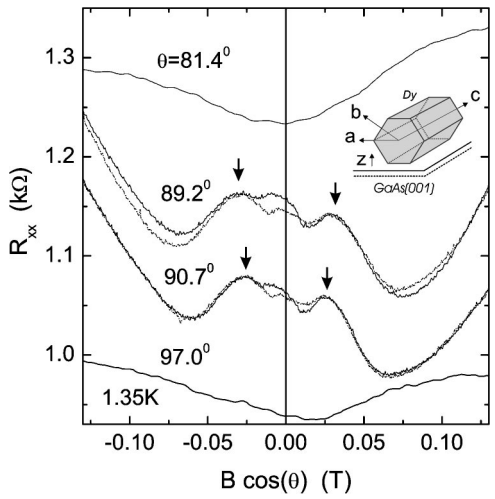

FIG. 5. Longitudinal resistance at grazing magnetic fields. The extra peak at $B_z \approx 0.03$ T ($B \approx 2.8$ T) is due to the coherent rotation of the magnetization (see text).

easy magnetic plane, defined by lattice vectors (**a**, **b**), grows perpendicular to the Dy/GaAs(001) interface. Dysprosium has a hcp crystal structure drawn in the inset to Fig. 5 with a hard magnetic axis in the *c* direction.[23] The *c*-axis parameter of 5.65 Å is lattice matched to GaAs(001) and the x-ray diffraction spectra of thin Dy/GaAs films have confirmed a texture in which the *c* axis grows in the plane of the interface.[11] At $\theta = 0°$, there is no energy cost involved in the magnetization reversal because the magnetic moments can rotate freely in the (**a**, **b**) plane. It is therefore not surprising that Fig. 2 shows no trace of magnetic hysteresis. In contrast, at grazing tilt angles $\theta \approx 90°$, the magnetoresistance shows an additional structure, indicated by arrows in Fig. 5, at $B_z \approx 0.03$ T ($B \approx 2.8$ T). This structure is symmetric about $\theta = 90°$ (see the $\theta = 89.2°$ and 90.7° traces) and is extremely sensitive to the tilt angle since it vanishes under a tiny misalignment comparable to the accuracy of our rotation probe. Grazing tilt angles augment the anisotropy energy[24] of the stripe by forcing a vector component of the magnetization along the *c* axis. At $\theta = 90°$, the magnetization reaches the equilibrium point at the top of the anisotropy barrier. This point is obviously unstable because it is possible for the magnetization to flip either up or down towards the easy plane. This realignment happens abruptly once the magnetostatic energy drops below the anisotropy barrier at $B \approx 2.8$ T. The instability disappears once the magnetic field is applied a few degrees off the plane so that magnetization reversal occurs smoothly (see the $\theta = 81.4°, 97.0°$ curves). The peak position at $B \approx 2.8$ T is comparable to the tabulated values of the coercive field of rare earths.[23,25]

In summary, tilted magnetic fields allow us to show that, in the limit of strong magnetic modulations, the Hall resistance measures the amount of electrons trapped by magnetic gradients. The electron drift path becomes increasingly localized into these regions as the 2DEG mobility decreases.

The support of EPSRC(UK) is gratefully acknowledged.

*Electronic address: A.R.Nogaret@bath.ac.uk

[1] A.K. Geim, S.V. Dubonos, J.G.S. Lok, I.V. Grigorieva, J.C. Maan, L.T. Hansen, and P.E. Lindelof, Appl. Phys. Lett. **71**, 2379 (1997).

[2] A.N. Grigorenko, S.J. Bending, T. Tamegai, S. Ooi, and M. Henini, Nature (London) **414**, 728 (2001).

[3] F.G. Monzon, M. Johnson, and M.L. Roukes, Appl. Phys. Lett. **71**, 3087 (1997).

[4] J. Reijniers and F.M. Peeters, J. Appl. Phys. **87**, 8088 (2000).

[5] F.M. Peeters and X.Q. Li, Appl. Phys. Lett. **72**, 572 (1998).

[6] F. Evers, A.D. Mirlin, D.G. Polyakov, and P. Wölfle, Phys. Rev. B **60**, 8951 (1999).

[7] K.S. Novoselov, A.K. Geim, S.V. Dubonos, Y.G. Cornelissens, F.M. Peeters, and J.C. Maan, Phys. Rev. B **65**, 233312 (2002).

[8] C.J.B. Ford, S. Washburn, M. Büttiker, C.M. Knoedler, and J.M. Hong, Phys. Rev. Lett. **62**, 2724 (1989).

[9] M.L. Roukes, A. Scherer, S.J. Allen, H.G. Craighead, R.M. Ruthen, E.D. Beebe, and J.P. Harbison, Phys. Rev. Lett. **59**, 3011 (1987).

[10] P. Ye, D. Weiss, R. Gerhardts, M. Seeger, K. von Klitzing, K. Eberl, and H. Nickel, Phys. Rev. Lett. **74**, 3013 (1995).

[11] D.N. Lawton, A. Nogaret, S.J. Bending, D.K. Maude, J.-C. Portal, and M. Henini, Phys. Rev. B **64**, 033312 (2001).

[12] Magnetic anisotropy is only evidenced at grazing tilt angles through a weaker separate peak in Fig. 5.

[13] J. Reijniers and F. Peeters, Phys. Rev. B **63**, 165317 (2001).

[14] A. Matulis and F. Peeters, Phys. Rev. B **62**, 91 (2000).

[15] A. Nogaret, S. Carlton, B. Gallagher, P. Main, M. Henini, R. Wirtz, R. Newbury, M. Howson, and S. Beaumont, Phys. Rev. B **55**, 16 037 (1997).

[16] J. Reijniers, F. Peeters, and A. Matulis, Phys. Rev. B **64**, 245304 (2001).

[17] H.-S. Sim, K.-H. Ahn, K.J. Chang, G. Ihm, N. Kim, and S. Lee, Phys. Rev. Lett. **80**, 1501 (1998).

[18] H. van Houten and C. Beenakker, *Solid State Physics* (Academic, New York, 1991), Vol. 44, p. 1.

[19] For computational purposes, the application of a tiny magnetic field (2 mT) turns extended trajectories forming the other 2/3 of the Fermi surface into periodic cyclotronic orbits.

[20] R. Gerhardts, Phys. Rev. B **53**, 11 064 (1996).

[21] A. Nogaret, S.J. Bending, and M. Henini, Phys. Rev. Lett. **84**, 2231 (2000).

[22] T.J. Thornton, M.L. Roukes, A. Scherer, and B.P.V. de Gaag, Phys. Rev. Lett. **63**, 2128 (1989).

[23] S. Legvold, *Ferromagnetic Materials* (North-Holland, Amsterdam, 1980), Vol. 1, p. 185.

[24] By anisotropy energy we refer to the magnetocrystalline anisotropy ($K = 87 \times 10^6$ J m^{-3}). Demagnetization effects are negligible since $\frac{1}{2}\mu_0 M_s^2 (n_\perp - n_\parallel) = -0.9 \times 10^6$ J m$^{-3} \ll K$ where $n_\perp = 0.285$ and $n_\parallel = 0.715$ are the demagnetization factors of the stripe.

[25] W.F. Brown, Rev. Mod. Phys. **17**, 15 (1945).